Nanostructured Biosensors Built by Layer-by-Layer Electrostatic Assembly of Enzyme-Coated Single-Walled Carbon Nanotubes and Redox Polymers

ARTICLE *in* LANGMUIR · DECEMBER 2006

Impact Factor: 4.46 · DOI: 10.1021/la060857v · Source: PubMed

5 AUTHORS, INCLUDING:

Pratixa Joshi
University of Texas at Austin
24 PUBLICATIONS **722** CITATIONS
SEE PROFILE

Matthew Johnson
University of Oklahoma
138 PUBLICATIONS **2,580** CITATIONS
SEE PROFILE

Langmuir **2006,** *22,*

Nanostructured Biosensors Built by Layer-by-Layer Electrostatic Assembly of Enzyme-Coated Single-Walled Carbon Nanotubes and Redox Polymers

Youdan Wang,[†] Pratixa P. Joshi,[‡] Kevin L. Hobbs,[§] Matthew B. Johnson,[§] and David W. Schmidtke*[,†,‡]

University of Oklahoma Bioengineering Center, School of Chemical, Biological and Materials Engineering, Homer L. Dodge Department of Physics and Astronomy, University of Oklahoma, 100 East Boyd, Norman, Oklahoma 73019

Received March 30, 2006. In Final Form: August 22, 2006

In this study, we describe the construction of glucose biosensors based on an electrostatic layer-by-layer (LBL) technique. Gold electrodes were initially functionalized with negatively charged 11-mercaptoundecanoic acid followed by alternate immersion in solutions of a positively charged redox polymer, poly[(vinylpyridine)Os(bipyridyl)$_2$Cl$^{2+/3+}$], and a negatively charged enzyme, glucose oxidase (GOX), or a GOX solution containing single-walled carbon nanotubes (SWNTs). The LBL assembly of the multilayer films were characterized by UV−vis spectroscopy, ellipsometry, and cyclic voltammetry, while characterization of the single-walled nanotubes was performed with transmission electron microscopy, Raman spectroscopy, thermogravimetric analysis, and X-ray photoelectron spectroscopy. When the GOX solution contained single-walled carbon nanotubes (GOX-SWNTs), the oxidation peak currents during cyclic voltammetry increased 1.4−4.0 times, as compared to films without SWNTs. Similarly the glucose electro-oxidation current also increased (6−17 times) when SWNTs were present. By varying the number of multilayers, the sensitivity of the sensors could be controlled.

Introduction

Due to their unique electrical, geometrical, fluorescent, and mechanical properties, single-walled carbon nanotubes (SWNTs) are attractive materials for the construction of nanoscaled biosensors. On the basis of these unique properties, several different biosensing platforms have been developed, such as SWNT-based electrochemical biosensors,[1−5] SWNT-based optical biosensors,[6,7] and SWNT-based electronic biosensors.[8,9] Although a variety of different biomolecules have been utilized in biosensor development, such as aptamers,[10] DNA,[11−13] enzymes,[14−16] and antibodies,[8,17,18] a majority of these biosensors have been developed for the enzymatic detection of glucose. SWNT-based biosensors for glucose have been fabricated by either adsorption[1,14,19] or covalent bonding of glucose oxidase (GOX) onto the SWNTs.[2,20] The detection schemes primarily utilized in SWNT-based glucose biosensors are electrochemical measurement of H_2O_2 production,[3,21,22] direct electron transfer from GOX,[1,2,20,23,24] electron transfer via diffusional[19,25] or immobilized mediators,[26,27] or fluorescent detection.[6,7]

The electrical "wiring" of redox enzymes to electrode surfaces by redox polymers is an attractive strategy not only for the development of reagentless biosensors[28−34] but also in the

* To whom correspondence should be addressed. E-mail: dschmidtke@ou.edu. Tel: (405) 325-7944. Fax: (405) 325-5813.

[†] University of Oklahoma Bioengineering Center.

[‡] School of Chemical, Biological and Materials Engineering.

[§] Homer L. Dodge Department of Physics and Astronomy.

(1) Guiseppi-Elie, A.; Lei, C. H.; Baughman, R. H. *Nanotechnology* **2002**, *13*, 559−564.

(2) Patolsky, F.; Weizmann, Y.; Willner, I. *Angew. Chem., Int. Ed.* **2004**, *43*, 2113-2117.

(3) Wang, J.; Musameh, M. *Analyst* **2003**, *128*, 1382−1385.

(4) Lin, Y. H.; Lu, F.; Tu, Y.; Ren, Z. F. *Nano Lett.* **2004**, *4*, 191−195.

(5) Wang, J. *Electroanalysis* **2005**, *17*, 7−14.

(6) Barone, P. W.; Parker, R. S.; Strano, M. S. *Anal. Chem.* **2005**, *77*, 7556−7562.

(7) Barone, P. W.; Baik, S.; Heller, D. A.; Strano, M. S. *Nat. Mater.* **2005**, *4*, 86−92.

(8) Chen, R. J.; Bangsaruntip, S.; Drouvalakis, K. A.; Kam, N. W.; Shim, M.; Li, Y.; Kim, W.; Utz, P. J.; Dai, H. *Proc. Natl. Acad. Sci. U.S.A.* **2003**, *100*, 4984−4989.

(9) Patolsky, F.; Zheng, G.; Hayden, O.; Lakadamyali, M.; Zhuang, X.; Lieber, C. M. *Proc. Natl. Acad. Sci. U.S.A.* **2004**, *101*, 14017−14022.

(10) So, H. M.; Won, K.; Kim, Y. H.; Kim, B. K.; Ryu, B. H.; Na, P. S.; Kim, H.; Lee, J. O. *J. Am. Chem. Soc.* **2005**, *127*, 11906−11907.

(11) Jeng, E. S.; Moll, A. E.; Roy, A. C.; Gastala, J. B.; Strano, M. S. *Nano Lett.* **2006**, *6*, 371−375.

(12) Kelley, K.; Pehrsson, P. E.; Ericson, L. M.; Zhao, W. *J. Nanosci. Nanotechnol.* **2005**, *5*, 1041−1044.

(13) Star, A.; Tu, E.; Niemann, J.; Gabriel, J. C.; Joiner, C. S.; Valcke, C. *Proc. Natl. Acad. Sci. U.S.A.* **2006**, *103*, 921−926.

(14) Gooding, J. J.; Wibowo, R.; Liu, J.; Yang, W.; Losic, D.; Orbons, S.; Mearns, F. J.; Shapter, J. G.; Hibbert, D. B. *J. Am. Chem. Soc.* **2003**, *125*, 9006−9007.

(15) Gan, Z. H.; Zhao, Q.; Gu, Z. N.; Zhuang, Q. K. *Anal. Chim. Acta* **2004**, *511*, 239−247.

(16) Rege, K.; Raravikar, N. R.; Kim, D. Y.; Schadler, L. S.; Ajayan, P. M.; Dordick, J. S. *Nano Lett.* **2003**, *3*, 829−832.

(17) O'Connor, M.; Kim, S. N.; Killard, A. J.; Forster, R. J.; Smyth, M. R.; Papadimitrakopoulos, F.; Rusling, J. F. *Analyst* **2004**, *129*, 1176−1180.

(18) Takeda, S.; Sbagyo, A.; Sakoda, Y.; Ishii, A.; Sawamura, M.; Sueoka, K.; Kida, H.; Mukasa, K.; Matsumoto, K. *Biosens. Bioelectron.* **2005**, *21*, 201−205.

(19) Azamian, B. R.; Davis, J. J.; Coleman, K. S.; Bagshaw, C. B.; Green, M. L. *J. Am. Chem. Soc.* **2002**, *124*, 12664−12665.

(20) Liu, Y.; Wang, M.; Zhao, F.; Xu, Z.; Dong, S. *Biosens. Bioelectron.* **2005**, *21*, 984−988.

(21) Wang, J.; Musameh, M.; Lin, Y. *J. Am. Chem. Soc.* **2003**, *125*, 2408−2409.

(22) Hrapovic, S.; Liu, Y. L.; Male, K. B.; Luong, J. H. T. *Anal. Chem.* **2004**, *76*, 1083−1088.

(23) Cai, C.; Chen, J. *Anal. Biochem.* **2004**, *332*, 75−83.

(24) Luo, X. L.; Killard, A. J.; Smyth, M. R. *Electroanalysis* **2006**, *18*, 1131−1134.

(25) Davis, J. J.; Coleman, K. S.; Azamian, B. R.; Bagshaw, C. B.; Green, M. L. *Chemistry* **2003**, *9*, 3732−3739.

(26) Callegari, A.; Cosnier, S.; Marcaccio, M.; Paolucci, D.; Paolucci, F.; Georgakilas, V.; Tagmatarchis, N.; Vazquez, E.; Prato, M. *J. Mater. Chem.* **2004**, *14*, 807−810.

(27) Joshi, P. P.; Merchant, S. A.; Wang, Y.; Schmidtke, D. W. *Anal. Chem.* **2005**, *77*, 3183−3188.

(28) Heller, A. *Acc. Chem. Res.* **1990**, *23*, 128−134.

(29) Csoregi, E.; Schmidtke, D. W.; Heller, A. *Anal. Chem.* **1995**, *67*, 1240−1244.

(30) Calvo, E. J.; Etchenique, R.; Danilowicz, C.; Diaz, L. *Anal. Chem.* **1996**, *68*, 4186−4193.

development of miniaturized biofuel cells.[35,36] Redox polymer-based biosensors have several advantages: (a) they do not require oxygen for their operation[37,38] (unlike sensors which measure either hydrogen peroxide formation or oxygen depletion); (b) their operating potential can be tuned by the appropriate chemistry;[39−41] (c) they exhibit high current densities (1 mA/cm^2);[42,43] (d) they have no leachable components; and (e) they are able to electrically communicate with several different enzymes.[33,37,39,44]

In order for these sensors to be commercially useful, methods are needed which allow for the controlled deposition of polymer and/or enzyme. Layer-by-layer (LBL) assembly is a simple technique which allows for the construction of nanoscale structured films by the sequential exposure of polycationic and polyanionic solutions.[45,46] Recently, several studies have demonstrated that the LBL technique can be combined with redox polymers or enzymes to form nanoscale structured biosensors.[47−53] However, the current density of these sensors is often low (<10 μA/cm^2).[47,48,54]

An alternative approach to fabricate nanoscale biosensors has been to combine the LBL technique with the unique electrical properties of carbon nanotubes. Sensors for dopamine[55] and cholesterol[56] have been developed by LBL assembly of negatively charged, multiwalled carbon nanotubes (MWNTs) and positively charged poly(diallyldimethylammonium chloride) (PDDA), while a sensor for choline was based upon multilayer films of MWNTs and polyaniline.[57] More recently, the LBL approach with carbon nanotubes has been utilized in the electrochemical detection of proteins and nucleic acids.[58]

Recently we reported that incorporation of enzyme modified SWNTs into redox polymer films, dramatically increased both the electrochemical and enzymatic response of the sensors.[27] Incorporation of SWNTs, modified with GOX, into the redox polymer films resulted in a 2−10-fold increase in the oxidation and reduction peak currents during cyclic voltammetry, while the glucose electro-oxidation current was increased 3-fold to $\sim$70 μA (or $\sim$1 mA/cm^2) for SWNT weight percents between 17.5 and 31.0 wt %. Similar effects were also observed when SWNTs were modified with horseradish peroxidase prior to incorporation into redox hydrogels, suggesting that this method may be applicable to other enzymes as well.

In this study we test the hypothesis that incorporation of SWNTs into the LBL assembly of redox polymer-based biosensors would enhance their sensitivity. To build LBL sensors, we utilized the method of Sirkar et al.,[48] where a gold electrode surface was first functionalized with the negatively charged 11-mercaptoundecanoic acid (MUA) and then alternatively exposed to solutions of positively charged redox polymer (PVP−Os), and negatively charged enzyme−SWNT solution. Incorporation of SWNTs lead to a dramatic (6−17-fold) increase in the current response which depended on the number of multilayers. Similarly, the electrochemical response measured by cyclic voltammetry was also increased (1.4−4-fold). The increased sensitivity of these films and the fact that the LBL technique is independent of electrode topology and size make them attractive materials as nanoscale building blocks for a number of novel applications. In the area of glucose sensing, they may be utilized in the development of fast, portable, and miniaturized biosensors for glucose determination in clinical, biological, and fermentation samples. Similarly, they may also be useful in the development of novel immunosensors[59−62] and DNA sensors[63,64] based on "wired" enzyme detection schemes.

Experimental Section

Chemicals and Solutions. GOX from *Aspergillus niger* (EC 1.1.3.4, type X-S, 179 units/mg solid, 75% protein), MUA, and D-glucose were all purchased from Sigma Chemical Co. (St. Louis, MO). All chemicals were used as received. The redox polymer, designated as PVP−Os, was synthesized by partially complexing the pyridine nitrogens of poly(4-vinylpyridine) with $Os(bpy)_2Cl^{+/2+}$ and then partially quaternizing the resulting polymer with 2-bromoethylamine according to a previously published protocol.[37] Phosphate-buffered saline solution (PBS), pH 7.4, was prepared from 8 g/L NaCl, 0.2 g/L KCl, 0.2 g/L KH_2PO_4, and 1.15 g/L Na_2HPO_4 in Nanopure deionized water. Stock solutions of 2 M glucose were allowed to mutarotate for 24 h so that the α and β forms of D-glucose could reach a final stable ratio of $\alpha/\beta = 36{:}64$ before use. All glucose concentrations reported are expressed as total D-glucose concentrations.

SWNTs Purification and Characterization. AP-grade SWNTs (diameter 15−17 Å) were purchased from Carbolex (Lexington, KY). According to the manufacturer, these samples contain both amorphous carbon and metal catalyst impurities (Ni, Y) encapsulated in carbon shells with a sample purity of 50−70 vol %. Thus, the raw SWNTs were purified by a two-step process to remove any catalyst

(31) Kulagina, N. V.; Shankar, L.; Michael, A. C. *Anal. Chem.* **1999**, *71*, 5093−5100.
(32) Feldman, B.; Brazg, R.; Schwartz, S.; Weinstein, R. *Diabetes Technol. Ther.* **2003**, *5*, 769−779.
(33) Revzin, A. F.; Sirkar, K.; Simonian, A.; Pishko, M. V. *Sens. Actuators, B* **2002**, *81*, 359−368.
(34) Narvaez, A.; Suarez, G.; Popescu, I. C.; Katakis, I.; Dominguez, E. *Biosens. Bioelectron.* **2000**, *15*, 43−52.
(35) Mano, N.; Mao, F.; Heller, A. *J. Am. Chem. Soc.* **2002**, *124*, 12962−12963.
(36) Mano, N.; Mao, F.; Shin, W.; Chen, T.; Heller, A. *Chem. Commun. (Cambridge)* **2003**, 518−519.
(37) Gregg, B. A.; Heller, A. *Anal. Chem.* **1990**, *62*, 258−263.
(38) Pishko, M. V.; Katakis, I.; Lindquist, S. E.; Ye, L.; Gregg, B. A.; Heller, A. *Angew. Chem., Int. Ed. Engl.* **1990**, *29*, 82−89.
(39) Ohara, T. J.; Rajagopalan, R.; Heller, A. *Anal. Chem.* **1994**, *66*, 2451−2457.
(40) Taylor, C.; Kenausis, G.; Katakis, I.; Heller, A. *J. Electroanal. Chem.* **1995**, *396*, 511−515.
(41) Mano, N.; Mao, F.; Heller, A. *Chem. Commun. (Cambridge)* **2004**, 2116−2117.
(42) Ye, L.; Katakis, I.; Schuhmann, W.; Schmidt, H. L.; Duine, J. A.; Heller, A. *Diag. Biosens. Polym.* **1994**, *556*, 34−40.
(43) Mao, F.; Mano, N.; Heller, A. *J. Am. Chem. Soc.* **2003**, *125*, 4951−4957.
(44) Niculescu, M.; Frebort, I.; Pec, P.; Galuszka, P.; Mattiasson, B.; Csoregi, E. *Electroanalysis* **2000**, *12*, 369−375.
(45) Lvov, Y.; Ariga, K.; Ichinose, I.; Kunitake, T. *J. Am. Chem. Soc.* **1995**, *117*, 6117−6123.
(46) Decher, G. *Science* **1997**, *277*, 1232−1237.
(47) Hodak, J.; Etchenique, R.; Calvo, E. J.; Singhal, K.; Bartlett, P. N. *Langmuir* **1997**, *13*, 2708−2716.
(48) Sirkar, K.; Revzin, A.; Pishko, M. V. *Anal. Chem.* **2000**, *72*, 2930−2936.
(49) Calvo, E. J.; Etchenique, R.; Pietrasanta, L.; Wolosiuk, A.; Danilowicz, C. *Anal. Chem.* **2001**, *73*, 1161−1168.
(50) Gao, Q.; Yang, X. *Chem. Commun. (Cambridge)* **2004**, 30−31.
(51) Calvo, E. J.; Wolosiuk, A. *Chemphyschem* **2005**, *6*, 43−47.
(52) Li, W. J.; Wang, Z.; Sun, C. Q.; Xian, M.; Zhao, M. Y. *Anal. Chim. Acta* **2000**, *418*, 225−232.
(53) Flexer, V.; Forzani, E. S.; Calvo, E. J.; Luduena, S. J.; Pietrasanta, L. I. *Anal. Chem.* **2006**, *78*, 399−407.
(54) Ram, M. K.; Bertoncello, P.; Ding, H.; Paddeu, S.; Nicolini, C. *Biosens. Bioelectron.* **2001**, *16*, 849−856.
(55) Zhang, M.; Gong, K.; Zhang, H.; Mao, L. *Biosens. Bioelectron.* **2005**, *20*, 1270−1276.
(56) Guo, M. L.; Chen, J. H.; Li, J.; Nie, L. H.; Yao, S. Z. *Electroanalysis* **2004**, *16*, 1992−1998.
(57) Qu, F.; Yang, M.; Jiang, J.; Shen, G.; Yu, R. *Anal. Biochem.* **2005**, *344*, 108−114.
(58) Munge, B.; Liu, G.; Collins, G.; Wang, J. *Anal. Chem.* **2005**, *77*, 4662−4666.
(59) Vreeke, M.; Rocca, P.; Heller, A. *Anal. Chem.* **1995**, *67*, 303−306.
(60) Lopez, M. A.; Ortega, F.; Dominguez, E.; Katakis, I. *J. Mol. Recognit.* **1998**, *11*, 178−181.
(61) Parellada, J.; Narvaez, A.; Lopez, M. A.; Dominguez, E.; Fernandez, J. J.; Pavlov, V.; Katakis, I. *Anal. Chim. Acta* **1998**, *362*, 47−57.
(62) Lu, B.; Smyth, M. R.; OKennedy, R.; Moulds, J.; Frame, T. *Anal. Chim. Acta* **1997**, *340*, 175−180.
(63) Caruana, D. J.; Heller, A. *J. Am. Chem. Soc.* **1999**, *121*, 4728−4728.
(64) Zhang, Y.; Pothukuchy, A.; Shin, W.; Kim, Y.; Heller, A. *Anal. Chem.* **2004**, *76*, 4093−4097.

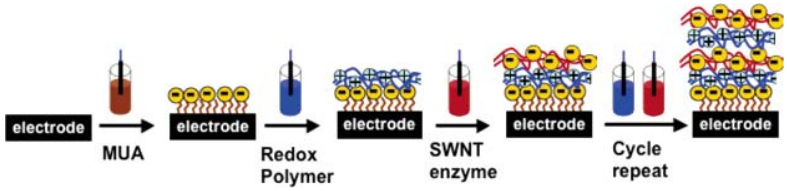

Figure 1. Schematic of the LBL film deposition process. Gold electrodes were first functionalized with the negatively charged thiol, 11-mercaptoundecanoic acid (MUA), and then alternatively incubated to solutions of positively charged redox polymer and negatively charged enzyme/SWNT.

or carbonaceous impurities. First, a low-temperature air oxidation was carried out at 350 °C for 30 min to remove any amorphous carbon. This was followed by refluxing in 4 M HCl for 18 h at 103 °C to remove any metal catalyst impurities. The samples were then washed with deionized water until the pH was neutral and then dried.

SWNTs were characterized by Raman spectroscopy, thermal gravimetric analysis (TGA), Fourier transform infrared spectroscopy (FTIR), X-ray photoelectron spectroscopy (XPS), and transmission electron microscopy (TEM). Samples for TEM were prepared by sonicating SWNTs in methanol and drop drying onto lacey carbon TEM grids and subsequently imaged with a JEOL JEM-2000FX TEM. Raman spectra were obtained with a Jobin Yvon-Horiba Lab Raman spectrometer with a CCD detector and 633 nm laser excitation. The extent of sidewall functionalization was evaluated by both TGA under argon and temperature programmed desorption (TPD) under helium. TGA was performed at Rice University with a thermogravimetric analyzer (Model SDT 2960, TA Instruments, New Castle, DE) by placing the sample in the furnace with an argon atmosphere and heating it at the rate of 10 °C/min up to 120 °C, holding at 120 °C for 30 min to remove any moisture, and then again heating it at the rate of 10 °C/min up to 850 °C. TPD was performed with an in-house-built unit as previously described.[65] Briefly, a known amount of SWNT sample was placed in a programmable temperature-controlled oven and heated in a linear temperature ramp up to 650 °C in flowing He. The exit stream from the oven was connected to a flame ionization detector (FID) which allowed for the detection and quantification of the desorbed species that evolved during the thermolysis. FTIR analysis of the functional groups present on the SWNTs was performed by grinding samples thoroughly with KBr and pressing into a pellet before being analyzed with a Bruker Equinox 55 FTIR spectrometer (Bruker Optics, Billerica, MA).

XPS was performed on SWNT samples that were purified by air oxidation alone (oxidized SWNTs), by air oxidation followed by HCl treatment (acid-treated SWNTs), and modified with GOX (GOX-SWNTs). SWNTs modified with GOX were prepared on quartz substrates by first dissolving GOX in a solution of acid treated-SWNTs and incubating for 18 h at 4 °C. The solution was then centrifuged at 13 000 rpm for 5 min with a microcentrifuge, and the supernatant was removed. Nanopure water was then added, and the SWNTs were resuspended by vortexing. This washing procedure was repeated two times to remove any unbound GOX. After being washed, the SWNTs modified with GOX were dispensed onto a quartz substrate and dried at room-temperature overnight. Control samples of oxidized SWNTs and acid-treated SWNTs were prepared in a similar procedure but without exposure to GOX. XPS measurements were recorded with a Physical Electronics PHI 5800 ESCA system with monochromatic Al Kα X-rays (photon energy of 1486.6 eV). The system was operated at 350 W and 15 kV with a background pressure of 2×10^{-9} Torr.

Preparation of LBL Films. Gold electrodes with diameters of 1.6 (Bioanalytical Systems, West Lafayette, IN) and 2.0 mm (CH Instruments) were first polished with 1 and 0.25 μm diamond polishing slurry on nylon polishing pads before being polished on microcloth pads with 0.05 μm alumina. Solutions of PVP−Os polymer (10 mg/mL in water), GOX (10 mg/mL in 20 mM MES buffer, pH 6), and GOX-SWNTs were used for sensor construction. The GOX-SWNTs solution was made by first preparing a highly concentrated suspension of acid-treated SWNTs (6.9 mg/mL) by weighing out ~34.5 mg of acid-treated SWNTs into a small vial and adding 5 mL of a 20 mM MES buffer solution (pH 6). The solution was then ultrasonicated for 30 min with an ultrasonic processor CPX750 (Cole Parmer). Next, GOX was adsorbed onto the acid-treated SWNTs by dissolving 10 mg of GOX in 1 mL of the SWNT suspension (6.9 mg/mL) and incubating for 18 h at 4 °C. To facilitate the adsorption of the positively charged redox polymer, a negatively charged layer of MUA was first deposited on the surface of the polished gold electrodes by immersing the electrodes in a solution of 1 mM MUA in ethanol for 20 min. The electrodes were then removed and washed with Nanopure deionized water. The electrodes were subsequently immersed in a polycationic solution of PVP−Os for 20min, washed with Nanopure deionized water to remove any excess material, and then immersed in a solution of GOX-SWNTs (10 mg/mL) for 40min. Multilayer films of PVP−Os/GOX-SWNT were then created by repeated alternating exposure to the redox polymer (PVP−Os) and enzyme (GOX-SWNT) solutions (Figure 1). As a control, we also fabricated multilayer films of PVP−Os/GOX by using GOX solutions (10 mg/mL) which did not contain any SWNTs.

UV−vis Spectrophotometry and Ellipsometry. To monitor the LBL assembly process and determine the thickness of the films formed, we utilized both UV−vis spectrophotometry and ellipsometry. For UV−vis spectrophotometry, we fabricated PVP−Os/GOX-SWNT and PVP/GOX multilayer films on quartz substrates. Absorption spectra were taken with a UV−vis spectrophotomer (UV-2101PC, Shimadzu) of multilayer films fabricated with and without acid-treated SWNTs. To determine the thickness of the films deposited during the LBL process, ellipsometric measurements were made on LBL films formed on gold-coated silicon wafers (100 nm Au layer on 5 nm of Cr on Si(111)) using a Gaertner L-117 manual ellipsometer (Gaertner Scientific Corp., Chicago, IL) at an angle of incidence of 60°. All measurements were made with a He−Ne laser at a wavelength of 632.8 nm, and all film thicknesses were calculated assuming a refractive index of 1.46 by Gaertner software.

Electrochemical Characterization. Cyclic voltammetry and constant potential measurements were performed with a CH Instruments bipotentiostat (CHI832, Austin, TX) in a three-electrode cell configuration with a saturated calomel reference electrode (SCE), and a platinum wire counter electrode. Constant temperature (25 ± 1 °C) was maintained during the experiments by using a water-jacketed electrochemical cell connected to a circulating water bath. Glucose calibration curves were obtained by adding aliquots of a stock 2 M glucose solution to a well-stirred cell with the working electrode poised at 500 mV vs SCE.

Calculations and Statistics. Values are presented as mean ± standard error of the mean (SEM) unless otherwise specified, and statistical significance was assessed when appropriate by a Student's t-test for paired data, with $P < 0.05$ considered as statistically significant.

Results and Discussion

SWNT Purification and Characterization. SWNTs made by the arc-discharge method normally contain both catalyst and carbonaceous impurities (i.e., amorphous carbon, graphite). Thus,

(65) Buffa, F.; Hu, H.; Resasco, D. E. *Macromolecules* **2005**, *38*, 8258−8263.

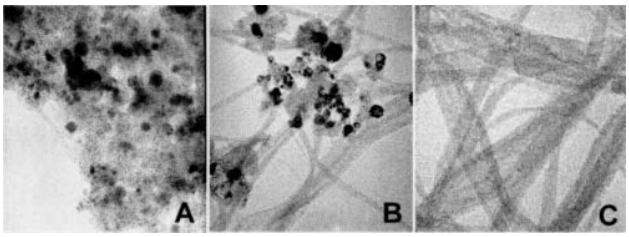

Figure 2. TEM images (a) raw SWNTs, (b) oxidized SWNTs, and (c) acid-treated SWNTs.

the first step in the construction of the LBL biosensors was to remove these impurities. SWNTs were purified by either an air-oxidation treatment alone or air oxidation treatment followed by a HCl reflux treatment. The purity of the SWNTs after the different purification steps was qualitatively assessed by TEM. Figure 2A shows that, prior to purification, the raw SWNTs contained a significant amount of metallic and carbonaceous impurities that covered the SWNTs bundles. Air oxidation of the raw SWNTs eliminated a majority of the carbonaceous impurities (Figure 2B), while subsequent reflux in HCl removed the metal catalyst particles (Figure 2C), leaving purified SWNT bundles.

The purity and structural integrity of the SWNTs during the purification process was also assessed by Raman spectroscopy, TGA, FTIR, and XPS. Figure 3 shows the Raman spectra of raw SWNTs, oxidized SWNTs, and acid-treated SWNTs. The shape of the G-bands at 1500−1600 cm^{-1} indicate the presence of SWNTs in each sample. The disordered D-band at 1300−1400 cm^{-1} is attributed to carbon defects and was used to evaluate the structural disorder in the SWNT samples. Figure 3B shows that air oxidation of the SWNT sample dramatically reduced the D-band and hence the amount of disordered carbon with respect to the raw sample. Subsequent HCl treatment of the SWNTs led to a slight increase in the D-band. Although the ratio of the D-band area relative to the G-band area for acid-treated SWNTs (0.1745) was higher then that of oxidized SWNTs (0.1084), it was still lower than the D-band/G-band ratio for raw nanotubes (0.2154). The D-band/G-band ratio is often used as a qualitative measurement of SWNT purity.[66,67] TGA, when performed under inert atmospheres, has been widely used to estimate the content of functional groups on SWNTs.[68,69] To determine the effects of the purification process on the structure and composition of the SWNTs, we performed TGA on SWNT samples that had been purified by air oxidation alone, and samples that had been air oxidized followed by HCl treatment (Supporting Information, Figure S-1). The TGA curve for the air-oxidized sample showed a 16.7 wt % loss corresponding to a calculated functionalization coverage of 1/19, while the sample treated with air oxidization followed by HCl treatment showed only a 4.1 wt % loss corresponding to a coverage of 1/88. We obtained similar results by TPD analysis under helium (data not shown). XPS analysis of the air-oxidized SWNT samples and the acid-treated SWNT samples demonstrated that the treatment with HCl reduced both the oxygen content and the amount of metal catalyst impurities (from 8% to ∼0.1%) (see Supporting Information Figure S-2 for XPS spectra). The loss of functionality and oxygen content upon HCl treatment is somewhat surprising and is currently under investigation. FTIR analysis of the oxidized SWNT and acid-

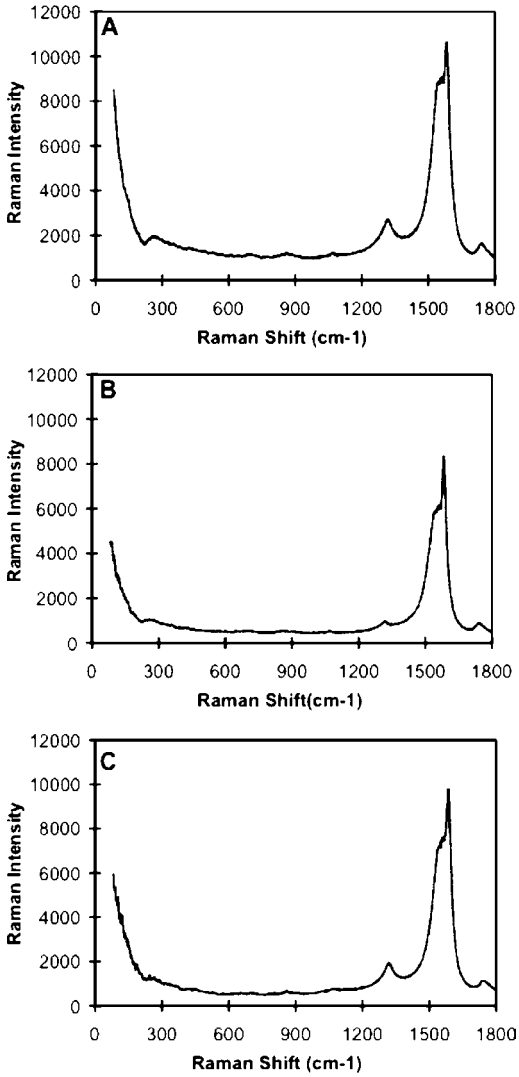

Figure 3. Raman Spectra for (A) raw SWNTs, (B) oxidized SWNTs, and (C) acid-treated SWNTs.

treated SWNT samples indicated the presence of hydroxyl groups and carboxylic acid groups on the tubes (data not shown). Taken together, these observations provide evidence that the purification process utilized eliminated a majority of the impurities and confirm the results of the TEM analysis.

To confirm that enzyme was adsorbing onto the SWNTs during the incubation step, XPS measurements were also performed on acid-treated SWNTs before and after GOX incubation. Figure 4A shows the XPS spectra for control acid-treated SWNTs and shows a predominant presence of carbon (96%) and oxygen (4%) via the detection of the C1s and O1s peaks. However, nitrogen (N1s peak) was undetected. In contrast, Figure 4B shows the spectra of acid-treated SWNTs incubated with GOX. Once again, carbon (77%) and oxygen (16%) are dominant; however, there is a distinct N1s peak at 400.3 eV for nitrogen (7%), which we assigned to nitrogen atoms that are present in the amide bonds in the enzyme's polypeptide chain. These results provide evidence that enzyme molecules were adsorbing onto the acid-treated SWNTs.

Characterization of the Multilayer Assembly Process. Amperometric biosensors for glucose were constructed by using a LBL self-assembly technique to sequentially deposit alternating layers of a positively charged redox polymer, Poly[(vinyl-pyridine)Os(bipyridyl)$_2$Cl$^{2+/3+}$ (PVP−Os), and a layer of GOX-

(66) Alvarez, W. E.; Pompeo, F.; Herrera, J. E.; Balzano, L.; Resasco, D. E. *Chem. Mater.* **2002**, *14*, 1853−1858.
(67) Chen, Y.; Ciuparu, D.; Lim, S. Y.; Yang, Y. H.; Haller, G. L.; Pfefferle, L. *J. Catalysis* **2004**, *225*, 453−465.
(68) Stephenson, J. J.; Hudson, J. L.; Azad, S.; Tour, J. M. *Chem. Mater.* **2006**, *18*, 374−377.
(69) Saini, R. K.; Chiang, I. W.; Peng, H.; Smalley, R. E.; Billups, W. E.; Hauge, R. H.; Margrave, J. L. *J. Am. Chem. Soc.* **2003**, *125*, 3617−3621.

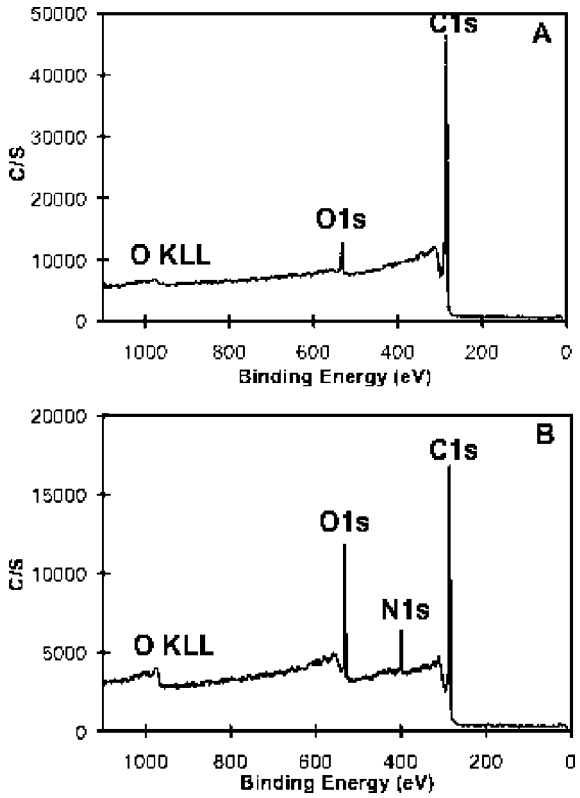

Figure 4. Survey X-ray photoelectron spectrum for (A) acid-treated SWNTs; and (B) acid-treated SWNTs incubated with GOX.

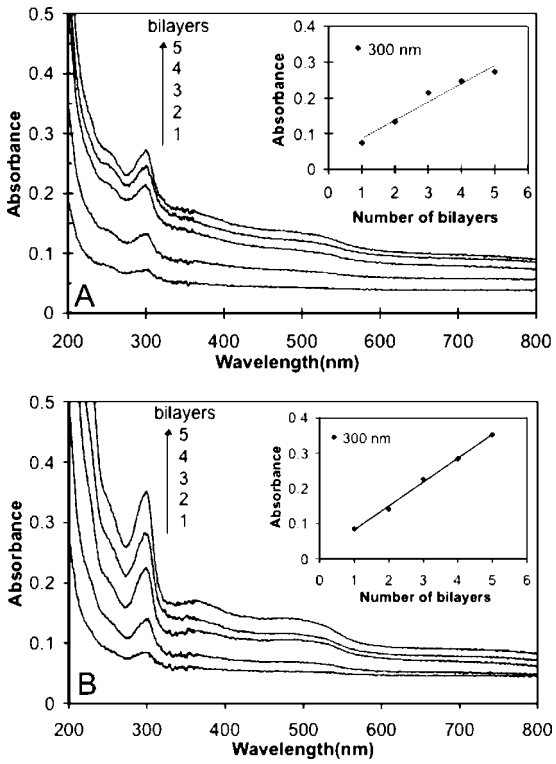

Figure 5. UV−vis aborption spectra for multilayer films on quartz slides. (A) Films made with SWNTs (i.e., PVP−Os/GOX-SWNT) and (B) films made without SWNTs (i.e., PVP−Os/GOX). The insets show the adsorption at 300 nm vs the number of bilayers.

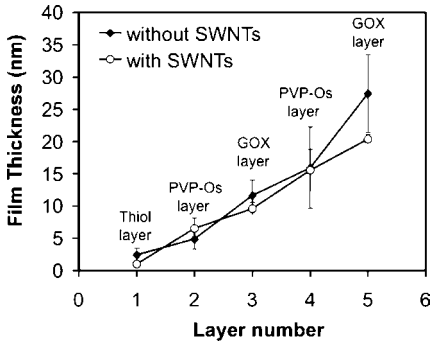

Figure 6. Plot of average film thickness upon deposition of each layer as measured by ellipsometry. (mean ± STD, n = 3−4 measurements).

coated SWNTs. GOX has an isoelectric point (pI) of 3.8 and thus possesses a net negative charge at pH 7.4.[70] To characterize and monitor the electrostatic self-assembly process, UV−vis absorption spectra were obtained from LBL films deposited on quartz slides and ellipsometric measurements were made on LBL films deposited on gold substrates. Figure 5A shows the spectra of films made with alternating layers of PVP−Os and GOX-SWNTs with different number of bilayers. We used the absorption at 300 nm, which was assigned to the $\pi-\pi^*$ transition of the bipyridine groups,[71] to measure the relative amount of PVP−Os deposited. The inset of Figure 5A shows the increase in absorption as a function of the number of bilayers deposited. The linear increase in absorbance with the number of bilayers suggests a uniform thickness of the bilayers deposited. As a control, we also deposited LBL films of the redox polymer PVP−Os and GOX without any SWNTs; the results of these films are shown in Figure 5B. Once again, an essentially linear dependence was found. Figure 6 shows the increase in the film thickness, as measured by ellipsometry, as subsequent layers were deposited during the LBL process. The thicknesses of films fabricated with and without GOX-SWNTs were nearly identical, which agrees with the UV−vis absorption data, and the average bilayer thickness of ∼10 nm is comparable with previous reports using similar redox polymers.[53,72]

Electrochemical Characterization. Cyclic voltammetry was performed to assess the effect of multiple layers on the electrochemical response and to investigate whether the incorporation of SWNTs into the multilayer films would increase the response. Figure 7A shows representative cyclic voltammograms (CVs) for electrodes made with 1, 2, 4, and 6 bilayers that contained no SWNTs. A pair of well-defined redox waves corresponding to the oxidation and reduction of the redox polymer's Os(bpy) complexes were observed at ∼300 mV vs SCE regardless of the number of bilayers deposited. Similarly, the peak potential separation (ΔE_p) was ∼40 mV for the different multilayer films, which suggests that the system was reversible. The current densities obtained were comparable to the results of other sensors built via the LBL assembly of redox polymers and enzymes.[33,47−49,53] The fact that the current response increased with each bilayer confirms the UV−vis absorption and ellipsometry data that additional redox polymer was deposited after each bilayer adsorption. Figure 7B shows the CVs obtained when GOX-SWNTs were incorporated into the multilayer films. Once again, a pair of well-defined redox waves were observed at ∼300 mV vs SCE and a ΔE_p of ∼35 mV was measured for the different multilayer films. These results suggest that the presence of SWNTs

(70) Chen, Q.; Kenausis, G. L.; Heller, A. *J. Am. Chem. Soc.* **1998**, *120*, 4582−4585.
(71) Sun, Y. P.; Sun, J. Q.; Zhang, X.; Sun, C. Q.; Wang, Y.; Shen, J. C. *Thin Solid Films* **1998**, *329*, 730−733.
(72) Forzani, E. S.; Otero, M.; Perez, M. A.; Teijelo, M. L.; Calvo, E. J. *Langmuir* **2002**, *18*, 4020−4029.

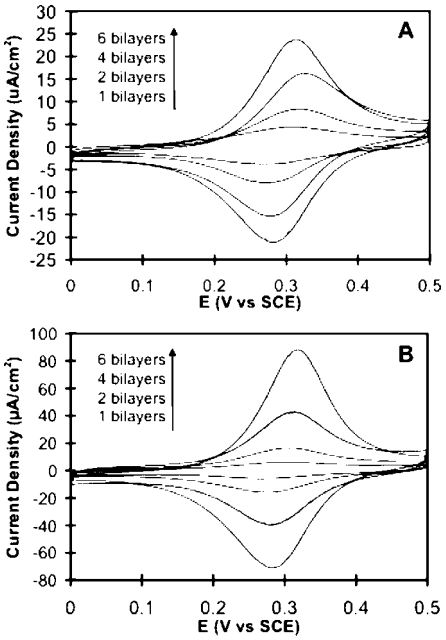

Figure 7. Effect of multilayers on electrochemical response. (A) Representative CVs of gold electrodes modified with 1, 2, 4, and 6 bilayers (PVP−Os/GOX) without SWNTs. (B) Representative CVs of gold electrodes modified with 1, 2, 4, and 6 bilayers (PVP−Os/GOX-SWNT) with SWNTs. Scan rates = 50 mV/s in PBS at 25 °C.

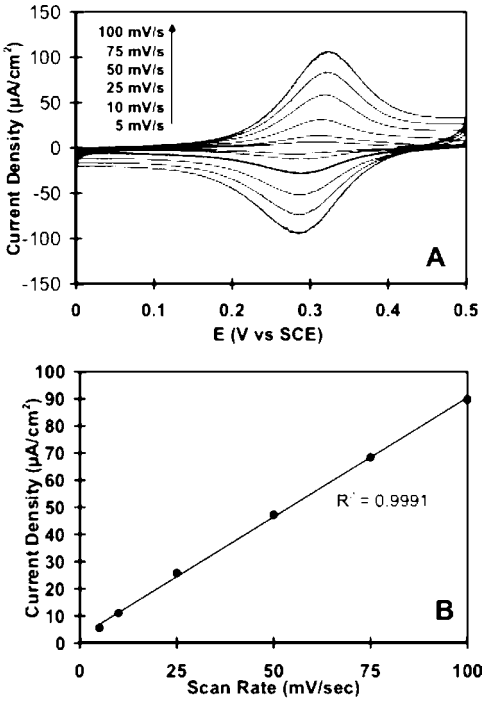

Figure 8. Effect of scan rate on electrochemical response. (A) Representative CVs of a gold electrode modified with four bilayers of PVP−Os/GOX-SWNT at different scan rates (5−100 mV/s) in PBS at 25 °C. (B) Plot of oxidative peak current with scan rate.

did not affect the reversibility of the system or the formal redox potential E_o. However, the incorporation of SWNTs into the films increased the electrochemical response of the sensors, increasing the peak currents from 2- to 4-fold for films with two bilayers and greater. For the case of a single bilayer, there was only a slight increase (1.35-fold) in the peak current.

To determine the amount of PVP−Os being deposited, we performed cyclic voltammetry in the absence of glucose at a slow scan rate (5 mV/s) and integrated the area under the anodic peak. The integrated charge for films formed with and without GOX-SWNTs increased linearly with each bilayer deposited (Figure S3 in the Supporting Information), and from these data, it was calculated that the amount of electroactive osmium redox sites present per adsorbed layer was 3.2×10^{-10} mol/cm^2 for films without SWNTs and 3.7×10^{-10} mol/cm^2 for films with SWNTs. Figure 8 shows the CVs obtained at different scan rates for a gold electrode coated with four bilayers of PVP−Os/GOX-SWNT. The fact that the peak separation was almost unchanged with scan rate and the linear dependence of the peak current with potential scan rate indicated a fast and reversible surface redox process.

The CV results agree with our previous study that demonstrated that the incorporation of SWNTs into redox polymer films enhanced the electrochemical response.[27] The exact cause of this increase is unknown at this time and is currently under investigation. In our previous study, we provided evidence that the presence of SWNTs in the films allowed for more osmium sites to become accessible in thick redox polymer films but that in very thin films there was no difference. In the current study, there was not much difference in the electrochemical response of electrodes made with a single bilayer. This seems logical since, in a single bilayer film, the amount of redox polymer adsorbed will only be dependent upon the negatively charged thiol layer that was first adsorbed onto the gold electrode. Thus, the presence of SWNTs in the GOX layer should not affect the amount of redox polymer adsorbed or the electron-transfer process from the redox polymer through the thiol layer to the gold surface. However, the presence of SWNTs in the outer GOX layer may influence the geometry/smoothness of the layer and thus promote more redox polymer to be adsorbed in subsequent layers when compared to multilayer films in which SWNTs are not present. The fact that the electrochemical response increased from 2- to 4-fold as the number of bilayers increased from $n = 2$ to $n = 6$, would suggest that more redox polymer was being incorporated. However, the UV−vis absorption, ellipsometry, and charge integration data for films made with and without SWNTs would suggest that this was not the case. An alternative possibility is that the presence of SWNTs allows for an increased rate of charge transfer through the films.[73] Normally, the rate of charge transport through redox polymers is a function of (a) the self-exchange rate between redox centers, (b) the diffusion of counterions, and (c) polymer segment mobility.[43,74,75] The presence of SWNTs in our films may increase the charge transport by either increasing the permeability of the films to counterions or providing an alternative electron transfer pathway, where an electron can be transferred from one osmium redox center to a distant redox center via electron transport through the SWNT. At this time, the exact mechanism is unknown and is currently under investigation in our lab.

Enzymatic Response. The enzymatic response of LBL multilayer films to glucose was investigated by cyclic voltammetry and constant-potential amperometry. Figure 9 shows the CVs of a gold electrode modified with four bilayers of PVP−Os/GOX-SWNTs in the absence and presence of 60 mM glucose. When no glucose was present, a reversible redox peak was observed at 300 mV. However, upon addition of 60 mM glucose, there was a substantial increase in the oxidation current and a

(73) Granot, E.; Basnar, B.; Cheglakov, Z.; Katz, E.; Willner, I. *Electroanalysis* **2006**, *18*, 26−34.
(74) Aoki, A.; Heller, A. *J. Phys. Chem.* **1993**, *97*, 11014−11019.
(75) Wang, B. Q.; Brown, S.; Rusling, J. F. *Electroanalysis* **2005**, *17*, 1601−1608.

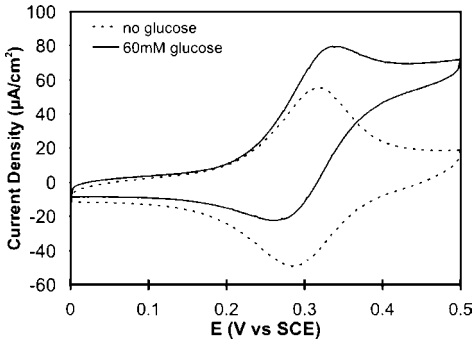

Figure 9. Response of sensor to glucose. CVs of a four bilayer film of PVP−Os/GOX-SWNT in PBS at 25 °C without glucose (− − −) and in 60 mM glucose (—). Scan rate = 50 mV/s.

concomitant decrease in the reduction current. This behavior is indicative of redox polymer mediation of the well-known GOX-catalyzed oxidation of glucose:[28,37]

$$\text{Glucose} + \text{GOX(FAD)} \rightarrow \text{gluconolactone} + \text{GOX(FADH}_2\text{)} \quad \text{(Reaction 1)}$$

$$\text{GOX(FADH}_2\text{)} + 2\text{PVP}-\text{Os}^{3+} \rightarrow \text{GOX(FAD)} + 2\text{PVP}-\text{Os}^{2+} \quad \text{(Reaction 2)}$$

$$\text{PVP}-\text{Os}^{2+} + \text{PVP}-\text{Os}^{3+} \rightarrow \text{PVP}-\text{Os}^{3+} + \text{PVP}-\text{Os}^{2+} \quad \text{(Reaction 3)}$$

$$\text{PVP}-\text{Os}^{2+} \rightarrow e^- + \text{PVP}-\text{Os}^{3+} \quad \text{(Reaction 4)}$$

where GOX(FAD) and GOX($FADH_2$) represent the oxidized and reduced forms of GOX, PVP−Os^{3+} and PVP−Os^{2+} represent the oxidized and reduced forms of the osmium bipyridine complexes of the redox polymer, Reaction 3 represents electron transfer between different osmium bipyridine complexes on the polymer, and Reaction 4 represents electron transfer from an osmium bipyridine complex to the electrode surface.

The response of the multilayer films, both with and without GOX-SWNTs, to glucose at 25 °C was investigated by poising the electrodes at 0.5 V vs SCE and measuring the output current as aliquots of a stock 2 M glucose were added to a well-stirred PBS solution (Figure 10). LBL sensors made without SWNTs (Figure 10A) displayed Michaelis−Menten-type behavior with an apparent K_m of ~9.3 mM. As the number of bilayers increased, the current output also increased. The current densities measured (10 μA/cm^2) compare favorably to previous studies involving LBL assembly of GOX and osmium[48,76] and ferrocene-based redox polymers.[47] Figure 10B shows the response of LBL sensors fabricated with SWNTs. Once again, Michaelis−Menten-type behavior was observed ($K_m \approx 10.4$ mM); however, the incorporation of the GOX-SWNTs into the nanocomposite structures resulted in a 6−17-fold increase in the steady-state current response depending on the number of multilayers.

The exact nature of this increased enzymatic response with SWNTs is unknown. As shown in Reactions 1−4, there are a number of events that can be rate limiting. If one assumes that there is no difference in the oxidation of glucose (Reaction 1) when SWNTs are present and that the rate of electron transfer to the electrode surface is fast (Reaction 4), then either the transfer of electrons from the enzyme's $FADH_2$ redox center to the polymer's osmium sites (Reaction 2) or the transfer of electrons

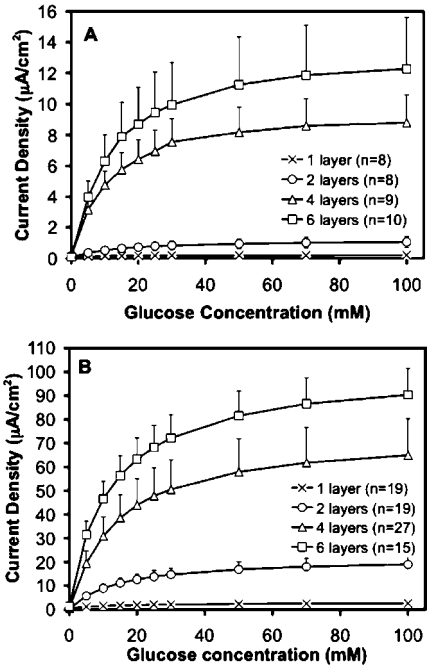

Figure 10. Effect of multilayer number on glucose response. Glucose calibrations curves for multilayer films constructed without (A) and with (B) SWNTs. All experiments were performed in PBS (pH 7.4) at $T = 25$ °C and $E = 0.5$ V vs SCE. (mean ± SEM)

through the redox polymer layer (Reaction 3) will be rate limiting. A recent study has suggested that the reoxidation of the GOX molecules in LBL redox polymer sensors is limited by the propagation of electrons through the multilayers.[77] The electrochemical results from Figure 7 clearly demonstrate that the presence of SWNTs affects the electrochemical response. However, the fact that the electrochemical response only increased 2−4-fold, while the enzymatic response increased from 6- to 17-fold would suggest that this is not the only factor. Furthermore, in the single bilayer film, there was little change (1.35-fold increase) in the electrochemical response with SWNTs while the enzymatic response was increased 10-fold. These results suggest that there is another factor involved.

An additional possibility is that the presence of SWNTs in the GOX layer allows for more of the enzyme molecules to be efficiently wired. Recent studies of LBL multilayer films constructed with redox polymers and GOX have suggested that only a small fraction of the total GOX molecules in a layer are electrically wired.[76,78] In addition, these studies have suggested that the fraction of enzyme wired depends on the ratio of osmium sites to enzyme molecules and that if one increases the amount of Osmium sites more enzyme is wired. Researchers have also shown that when GOX was adsorbed onto carbon nanotubes direct electron transfer with its buried FAD center, which is normally inaccessible, was possible.[1,20,23,24] It has been suggested that the distance between the FAD center and the underlying electrode surface is reduced below the normal distance of 13 Å due to either (a) partial unfolding of glucose oxdiase as it adsorbs onto the nanotube[79,80] or (b) the nanotube being able to penetrate closer to the FAD center due to its small diameter.[1,20] Similarly,

(76) Calvo, E. J.; Danilowicz, C. B.; Wolosiuk, A. *Phys. Chem. Chem. Phys.* **2005**, *7*, 1800−1806.
(77) Calvo, E. J.; Danilowicz, C.; Wolosiuk, A. *J. Am. Chem. Soc.* **2002**, *124*, 2452−2453.
(78) Calvo, E. J.; Wolosiuk, A. *Chemphyschem* **2004**, *5*, 235−239.
(79) Liu, J. Q.; Paddon-Row: M. N.; Gooding, J. J. *J. Phys. Chem. B* **2004**, *108*, 8460−8466.
(80) Zhao, Y. D.; Zhang, W. D.; Chen, H.; Luo, Q. M. *Anal. Sci.* **2002**, *18*, 939−941.

other studies have demonstrated that when proteins adsorb onto single-walled nanotubes, the structure and function of the proteins can be altered[81] and in some cases stabilized[82] by suppressing unfavorable protein−protein interactions. In our system, the first enzyme layer is separated from the gold electrode surface by a thiol layer and a redox polymer layer, thus even at its closest point, the likelihood that SWNTs are mediating direct electron transfer between the enzyme and the gold surface is low. However, it is possible that the enzyme becomes partially unfolded when incubated with nanotubes, which allows for improved access to the FAD centers by the osmium redox centers. At this time, we cannot rule out any of these possibilities, work is under way to determine the exact mechanism.

Conclusions

Nanoscaled multilayer films sensitive for glucose were fabricated by the LBL assembly of a polycationic redox polymer PVP−Os and the negatively charged enzyme GOX on gold electrodes. The self-assembly buildup of multilayer films was followed by UV−vis spectroscopy, ellipsometry, and cyclic voltammetry, while XPS measurements provided evidence of enzyme adsorption onto SWNTs. Both the electrochemical and enzymatic responses of the sensors could be controlled by varying the number of bilayers during the fabrication process. Incorporation of SWNTs into the LBL films did not appear to affect the redox potential of the films (∼300 mV) or the reversibility of electron transfer ($\Delta E_p = \sim 35$ mV). However, incorporation of SWNTs into structures with more than one bilayer did result in a 2−4-fold increase in the electrochemical response, while the enzymatic response to response to glucose was increased 6−17-fold. The increased current densities (∼90 μA/cm^2) exhibited by the films which had SWNTs incorporated in them should allow for the construction of sensors with reduced dimensions. Work is currently underway in our laboratories to determine the exact mechanism by which SWNTs increase the sensor's sensitivity and to apply this strategy to other redox enzymes (e.g., peroxidase, lactate oxidase) as well.

Acknowledgment. This work was supported in part by a NSF EPSCoR Grant (EPS-0132534), a NSF Career Award to D.W.S. (BES-0547619), and a U.S. Department of Energy grant (DE-FG02-06ER64239). The authors would also like to thank Dr. Yongqiang Tan for assistance with some of the Raman measurements, Mr. Stephen Merchant and Dr. Zhongrui Li for assistance with the XPS measurements, Mr Steven Crossley for assistance with the TPD measurements, and Rice University for access and assistance with the TGA measurements.

Supporting Information Available: Additional spectra and data. This material is available free of charge via the Internet at http://pubs.acs.org.

LA060857V

(81) Karajanagi, S. S.; Vertegel, A. A.; Kane, R. S.; Dordick, J. S. *Langmuir* **2004**, *20*, 11594−11599.

(82) Asuri, P.; Karajanagi, S. S.; Yang, H. C.; Yim, T. J.; Kane, R. S.; Dordick, J. S. *Langmuir* **2006**, *22*, 5833−5836.